

AI-Based Surface Composites and Strengthening Of Welded Joints Through Multi-Pass FSP Technique: A Review

Velaphi Msomi¹, Sipokazi Mabuwa¹, Ali Merdji²

¹Cape Peninsula University of Technology, Faculty of Engineering and the Built Environment, Mechanical Engineering Department, P.O. Box 1906, Bellville, 7535, South Africa, msomiv@gmail.com; sipokazimabuwa@gmail.com

²Faculty of Engineering and Technology, Mascara University, Algeria, merdji_ali@yahoo.fr



ABSTRACT

Friction stir processing (FSP) is a microstructural modifying technique that uses the same principles as the friction stir welding technique. FSP technique can be employed on the same surface repeatedly as desired and this repetition is called multi-pass friction stir processing (MFSP). The recent developments have shown that MFSP technique is very useful towards uniform dispersion of reinforcement particles during fabrication of surface composites. Some studies have also demonstrated that MFSP technique can be employed on welded joints as a way of improving the mechanical properties of the welded joints. This paper reports on the progress made in using the multi-pass friction stir processing (MFSP) technique in producing aluminium-based surface composites. It further looks at the progress made in using the MFSP on aluminium-based welded joints. An effort is made to identify the gap that requires some exploration for the better utilization and understanding of this technique.

Key words: Tensile strength; ductility; microstructure; similar welded joints; dissimilar welded joints

1. INTRODUCTION

The use of aluminum alloys has increased over the years due to multiple ranges of its applications. This includes automobile body building, aerospace, marine, shipbuilding, food packaging, and many other structural applications [1] – [3]. The interest in the use of aluminum alloys is based on appealing characteristics like high strength to weight ratio, appearance, higher ductility, and ease of fabrication [4], [5]– [7]. Various aluminum alloys behave differently due to the different alloying elements used to produce them [8] – [10]. However, it is a well-known fact that material improvements are very essential for better performance as well as for increasing the life span of components [11]. There are many material enhancing techniques that are available in the literature and amongst those techniques friction stir processing is counted as one of them [12] – [14].

Friction stir processing (FSP) is an emerging microstructural modifying technique that uses similar principle as friction stir welding (FSW) to process materials

in various ways besides joining them [8], [13], [15], [16]. The two techniques use similar parameters but working with different surfaces, i.e., FSW works on two base metals while FSP operates on a single surface. FSP technique was initially looked as the generic tool for microstructural refinement that has the capabilities of eliminating microstructural defects and thereby improving various properties of a material [17]. The performance of FSP involves softening of the material due to the heat generated from the rotating pin and the surface being processed. The penetration depth is being determined by the pin probe and the shoulder of the tool. The contact between the surface and the rotating shoulder of the tool acts as the extra source of heat that is required to plasticize the material around the inserted pin [18] – [21].

The role played by the tool shoulder is to forge the metal that flows upward due to the stirring action of the pin. The tool moves relative to the area being processed during the FSP process [21]. Figure 1 shows a schematic diagram of the FSP technique. As a result of the heat generation and severe plastic deformation during the FSP process, the uniformly distributed refined grains are achieved. This, therefore, results in mechanical properties being affected dramatically. A typical example includes the work of Mehdi and Mishra [18] where the impact of employing FSP on the TIG welded dissimilar joint was analyzed. The decrease in grain size was found to be related to the tool pin parameters. It was discovered that the specimens with the refined grains exhibited higher tensile stress, percentage elongation, and microhardness compared to the TIG welded specimens. It was also discovered that the rotational and traverse speed have a major influence on the mechanical properties of the processed specimens.

The other typical example includes the effect of employing the FSP technique on AA5005-H34 and AA7075-T651 [19]. Different pin profiles (square-base canonical head – Tool 1, square cross-section cylindrical- Tool 2, and screw-threaded canonical- Tool 3) were used with different processing parameters. The processing of AA5005 involved the use of Tool 1 and Tool 3 with three different rotational speeds and constant traverse speed (127 mm/min). The AA7075 was processed with all three pins using varying rotational speed and traverse speed. The decrease in grain size with an increase in rotational speed was observed in all the processed specimens. However, it was observed that the grain refinement did not translate to improved mechanical

properties as both materials behave differently under different temperatures. The increase in rotational speed in processing AA50005 using both Tool 1 and Tool 3 resulted in the drop in ultimate tensile strength (UTS) and microhardness. The percentage elongation for specimens produced using Tool 1 showed a growing trend from the rotational speed of 490 rpm till 970 rpm which then followed by a significant drop beyond 970 rpm. However, the percentage elongation for specimens produced using Tool 3 showed a growing trend from the low rotational speed until the highest rotational speed (1200 rpm). The processing of AA7075 was based on three different pin profiles coupled with four different rotational speed and traverse speed. The increase in microhardness was observed between the rotational speed of 490 rpm and 970 rpm and the significant drop followed beyond 970 rpm for all specimens produced using the three-pin profiles. However, the microhardness showed a growing trend from the lowest until the highest traverse speed. The increase in rotational speed resulted in a decrease in UTS, whereas an increase in traverse speed resulted in an improved UTS and yield strength of the processed specimens. However, the mechanical properties of all processed specimens remained lower than the parent materials. The best mechanical properties for AA5005-H34 were obtained when Tool 3 was used with the rotational speed between 970 rpm and 1200 rpm.

Nelaturu *et al.* [20] have investigated the impact of the FSP technique on the fatigue life of A356 aluminum alloy. The performance of FSP was based on two rotational speed (300 rpm and 1500 rpm) with a constant traverse speed (102 mm/min), which was then followed by heat treatment. The employment of FSP resulted in the modification of the dendritic microstructure and the redistribution of Si particles. The specimens produced at high rotational speed had coarser grains compared to those produced at low rotational speed. The specimens with finer grains exhibited low tensile properties compared to other specimens and this was due to a high percentage of low angle grain boundaries (LAGB). The percentage elongation for all specimens was relatively the same (approximately 20%). The specimens with coarser grains exhibited higher fatigue life compared to those with finer grains, of which this was found to be contrary to the norm and the main contributing factor was found to be the difference in crack initiation and crack propagation. The work by Yang *et al.* [21] and Patel *et al.* [22] are some of the examples that also show the impact of employing the FSP technique on aluminum alloys to achieve refined grains which then influence the mechanical properties.

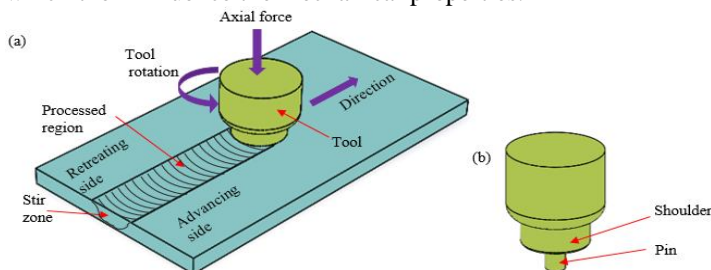


Figure 1: (a) Schematic diagram of the FSP technique and (b) FSP Tool.

FSP has been demonstrated to be an effective technique to acquire major granular refinement, densification, microstructural homogeneity of the processed zone, and microstructural defects elimination from metals. Some examples include the works by Santella *et al.* [23] where the FSP was employed on A356 aluminum alloy to reduce the porosity in the material. The overlapping FSP passes were performed based on a cylindrical pin with a hemispheric tip coupled with constant rotational speed (1000 rpm) and traverse speed (1.7 mm/s). The microstructural morphology revealed that the porosities observed in the unprocessed specimens were closed post FSP and the large second-phase particles were reduced and uniformly distributed throughout the processed zone. The uniform distribution of the second-phase particles and the elimination of porosity resulted in a more than 100% increase in percentage elongation and the ultimate tensile strength, i.e., percentage elongation increased from below 1% to above 12%; UTS increased from 151.5 MPa to above 300 MPa. Another example includes the work by Yadav and Bauri [24] where they analyzed the influence of FSP on the microstructural morphology of commercially pure aluminum. The performance of the FSP procedure was based on a constant rotational speed (640 rpm) and constant traverse speed (150 mm/min). The average grain size of base metal (84 μm) was significantly reduced to approximately 3 μm post FSP. The refined grains contributed to the enhancement of yield strength (from 35 MPa to 82 MPa and UTS (from 72 MPa to 90 MPa). However, a slight drop in percentage elongation (approximately 10% drop) was observed. The microhardness was also improved and the improvement was attributed to the major grain refinement in the processed region.

The work by Qin *et al.* [25] is another example that demonstrates that the FSP technique can be used to refine majorly the grain size. They analyzed the impact of FSP parameters on the microstructure and mechanical properties of Al-Mg₂Si. The threaded-conical tool pin profile coupled with a constant traverse speed (60 mm/min) and varying rotational speed (300 rpm – 1200 rpm) was utilized in performing the investigation. The increase in rotational speed from 300 rpm to 700 rpm resulted in an elimination of defect area, while further increase in rotational speed yielded the opposite results. However, the increase in rotational speed resulted in the formation of refined particles from the breakage of coarsened Mg₂Si dendrites. There was a notable increase in UTS and percentage elongation from 300 rpm until 700 rpm and a declining trend was observed after 700 rpm. This decline correlates with the phenomenon of microstructural defects observed during microstructural analysis. A similar increase and declining behavior were also observed during the microhardness analysis.

Processed surfaces have possessed enhanced properties like hardness, tensile strength, fatigue, corrosion, and wear resistance [24], [26] – [29]. One of the recent works on corrosion enhancement through the FSP technique includes the work by Liu *et al.* [26]. The circular truncated cone tool profile was used to perform FSP on AZ31 magnesium alloy

using varying high rotational speed (1000 rpm – 5000 rpm) and varying traverse speed (25 mm/min – 125 mm/min). The mean grain size for $Al_{12}Mg_{17}$ precipitates was found to be increasing with an increase in rotational speed and traverse speed, however, it was relatively smaller compared to the base metal. It was also observed that the homogeneous distribution of $Al_{12}Mg_{17}$ precipitates improved with an increase in rotational speed and traverse speed. The homogeneous distribution of these precipitates resulted in an improved corrosion potential (-1.563 V to -1.200 V) and corrosion current (1.55×10^{-4} A to -2.77×10^{-5} A). The microhardness of the stir zone was found to be decreasing with the increase in rotational speed and traverse speed, and this decline was attributed to the grain size increase observed during the microstructural analysis. The tensile properties were found to be stabilized (matching those of the base metal) when the tool rotational speed of 3000 rpm is used with a traverse speed of 75 mm/min.

Another typical example is the work of Ma et al. [27] where the FSP technique was employed on 2507 duplex stainless steel to analyze the corrosion behavior. The tapered tool pin profile was used with a constant rotational speed (400 rpm) and varying traverse speed (50-200 mm). There was a notable decrease in grain size with an increase in traverse speed, however, the increase in grain size was observed beyond the traverse speed of 100 mm/min. The microhardness followed the very same trend observed with microstructural analysis, with high microhardness for the specimen produced with a traverse speed of 100 m/min. The UTS was found to be increasing with an increase in traverse speed until 100 mm/min and started to drop beyond this traverse speed. The corrosion resistance was improved with the increase in traverse speed until 100 mm/min and the declining trend was observed beyond this traverse speed. The improvement in corrosion resistance with grain refinement is caused by the promotion of element diffusion, which results in the stability of the passivation film.

Sharma et al. [28] have demonstrated that FSP can be used to enhance the fatigue behavior of A356 aluminum alloy. The triflute pin profile was used to process one plate with a rotational speed of 700 rpm and a traverse speed of 203.2 mm/min, whereas the standard FSW pin with a rotational speed of 900 rpm and traverse speed of 203.2 mm/min was used in processing the other plate. The microstructural pores observed on the base metal diminished post FSP technique for both pins. The uniform distribution of refined Si particles was also observed post FSP procedure. The refinement and uniform distribution of Si particles resulted in an increase in fatigue strength threshold stress. The work of Jana et al. [29] is another example that demonstrates that FSP can affect the fatigue life of cast Al-Si-Mg alloy. The conical pin featured with a stepped spiral was used in conducting the FSP procedure. The rotational speed and traverse speed were fixed at 2236 rpm and 2.33 mm/s. The specimens subjected to FSP exhibited an improved fatigue life compared to as-cast specimens. There was also a significant increase in percentage elongation for the processed specimens compared to as-cast specimens.

The majority of FSP studies have investigated the effect of process parameters on the properties of the processed surface using a single pass. However, multi-pass friction stir processing (multi-pass FSP) is another method to further modify the microstructure of materials. This paper reviews the utilization of multi-pass FSP to fabricate surface composites and to enhance the various properties of single surface/plate and similar or dissimilar welded joints. Attention is paid more to the literature that revolves around the employment of the multi-pass FSP technique to enhance the welded similar and dissimilar joints produced from soft materials. An effort has been made to identify the gap that requires exploration regarding this technique.

2. COMPETENCES OF MULTI-PASS FRICTION STIR PROCESSING TECHNIQUE

Multi-pass friction stir processing (multi-pass FSP) can be employed to fabricate surface composites, modify the microstructure of the single surface or plate, and welded joints. Figure 2 shows the most critical parameters that are critical in multi-pass FSP during the fabrication of surface composites or improving the plate properties or to strengthen the welded joints. The employment of multi-pass FSP to fabricate surface composites is discussed in the subsequent section and this is followed by the employment of the same technique to enhance the properties of the single plate. The last section is discussing the application of the multi-pass FSP technique to strengthen similar or dissimilar welded joints.

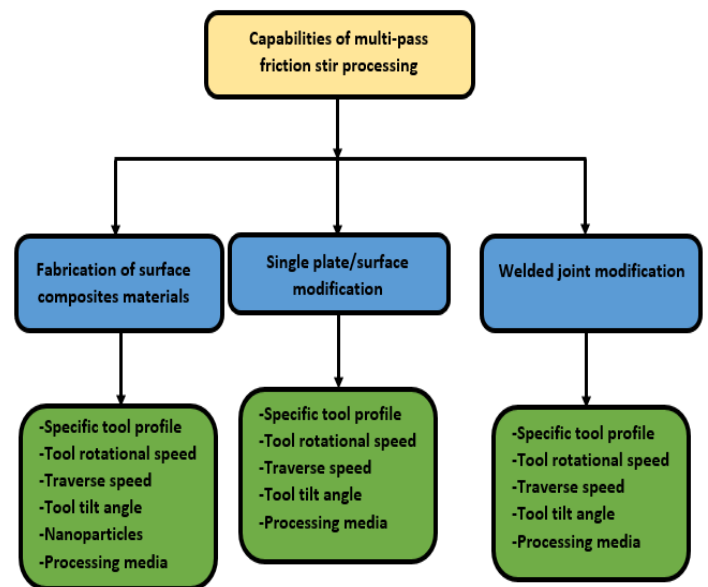


Figure 2. Competences of multi-pass friction stir processing technique.

2.1. Fabrication of Surface Composites Using Multi-Pass FSP Technique

Surface composites refer to the reinforcement of powdered materials (called particles) onto the surface of metals through

the use of friction stir processing (FSP) technology. The utilization of FSP technology has expanded such that a new method called multi-pass FSP has been reported. This section reviews the aluminum alloys that have been used in fabricating surface composites through the multi-pass FSP technique.

2.1.1. Fabrication of Surface Composites using AA1xxx

Recent developments have demonstrated that AA1xxx series can be used as the base metal in fabricating hybrid surface composites. The typical generic setup used in fabricating surface composites is shown in Figure 2. The initial step before multi-pass FSP is generally the enclosure of the holes filled with reinforcement particles using pin-less tool. This procedure is applied to avoid escaping of reinforcement particles during the processing or fabrication of surface composites. The generic resulting zones post multi-pass FSP are shown in Figure 3. These zones have different grain morphology, however, the main focus of analysis is always on the stir zone. This section reviews the works that have utilized AA1xxx series in fabricating surface composites via multi-pass FSP technique.

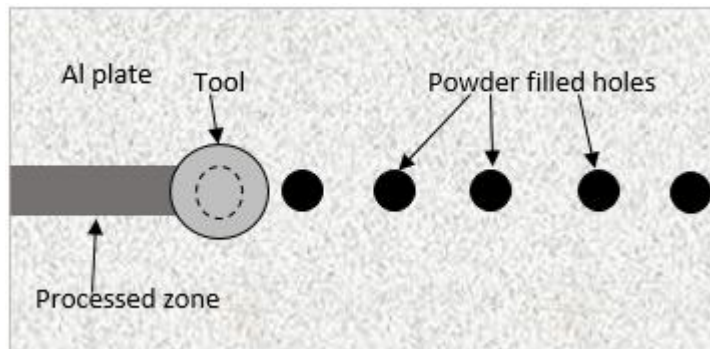


Figure 2. Schematic diagram depicting fabrication of surface composites setup

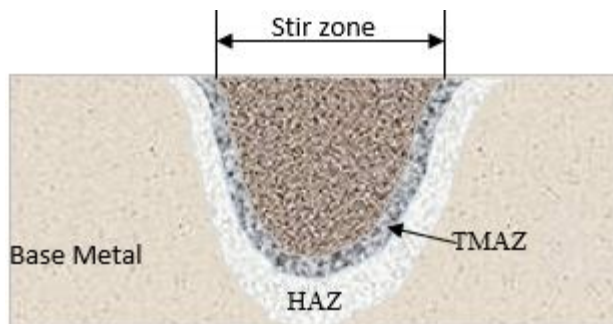


Figure 3. The side view of the processed joint depicting different microstructural zones

The recent work by Alishavandi *et al.* [30] have utilized a multi-pass FSP technique to fabricate surface hybrid in-situ aluminum matrix nanocomposites from AA1050 (base metal) reinforced with the mischmetal oxide nano-particles. The tool

rotational speed of 1600 rpm and a traverse speed of 100 mm/min were used for conducting multi-pass FSP. The pin-less tool was firstly used to enclose the reinforcements in the base metal, while the threaded cylindrical pin profile was utilized to carry out the six FSP passes. It should be noted that the multi-pass FSP was conducted with and without the reinforcements. The increase in the number of FSP passes without reinforcement yielded the refined grains (mean grain size of 30 μm), however, the incorporation of reinforcement particles assisted with further grain refinement (average size of 10 μm).

It was discovered that the increase in the number of FSP passes resulted in the uniform distribution of reinforcement particles and the reduction of agglomerated particle size. The microhardness of the 6-pass specimens processed without reinforcement (6PA) was 2 times higher than that of base metal (17 HV), while the 6-pass specimens processed with the incorporation of reinforcement (6PPA) resulted in the microhardness that was 2.6 times higher than the base metal. The spikey microhardness increase (3.4 times higher than the base metal) was observed on a 2-pass and 4-pass specimens processed with the inclusion of reinforcement (2PPA and 4PPA) and this increase was attributed to the inhomogeneous discontinuous dynamic recrystallization (DDRX) and nanoparticles agglomeration. The UTS and yield strength of 6PPA was 2.2 and 2.7 times higher than those of the base metal and 6PA specimens. However, the percentage elongation of 6PPA was found to be approximately 35% lower than that of the base metal and 6PA specimen. The increase in UTS and yield strength was attributed to a repeated refinement of grains and the DDRX synergistic effect.

The multi-pass FSP technique was employed to reinforce Al-Fe₃O₄ particles on the surface of AA1050 to produce hybrid surface nanocomposites [31]. The pin-less tool was used to enclose the reinforcement before processing and the reinforcement enclosure was conducted using a constant rotational speed of 1120 rpm and a traverse speed of 125 mm/min. The 4-pass FSP procedure was conducted using a cylindrical threaded pin based on a fixed rotational speed and traverse speed (1400 rpm and 40 mm/min, respectively). The properties of the hybrid surface nanocomposite were studied comparatively with the base metal and the processed surface without reinforcement. The multi-pass FSP procedure without resulted in the refined grains with a mean grain size of approximately 8 μm and the incorporation of reinforcements brought further grain refinement with a mean grain size of 2 μm . The further grain refinement post reinforcement addition was attributed to the grain boundary pinning mechanism resulted from the reaction of Al and Fe₃O₄. It was discovered that the high rotational speed used for processing triggered chemical reactions which influenced the microstructural evolutions which are key in the bulk material properties. The transformation of low angle grain boundaries (LAGBs) to high angle grain boundaries (HAGBs) of both processed and nanocomposite specimens was observed and the occurrence of this transformation was attributed to the continuous dynamic recovery. It is anticipated that the mechanical properties of Al-Fe₃O₄ based

nanocomposite can be improved. The improved mechanical properties of this nanocomposite were attributed to the high transformation of LAGBs to HAGBs [20].

The wear and corrosion behavior of the hybrid surface nanocomposites fabricated from AA1050 and mischmetal oxide (MMO) particles was studied by Alishavandi *et al.* [32]. The 6-pass FSP technique was used in fabricating hybrid surface composites and the processing of base metal (AA1050). The processing and fabrication were performed using a threaded cylindrical tool pin profile based on a fixed rotational speed and traverse speed (1600 rpm and 100 mm/min, respectively). The grains of the 6-pass composite specimen (6PPA) were finer compared to those of the base metal and the 6-pass processed specimen (6PA). The refined grains of 6PPA were attributed to the presence of MMO particles which enhanced the nucleation kinetics and nucleation sites. The presence of MMO particles also played a role in the hindrance of new grain boundary formation, which resulted in smaller grains with high dislocation density and HAGBs. The mechanical properties of the composites, processed specimens, and base metal behaved in the same manner observed in [30]. The wear resistance and corrosion resistance of 6PPA were found to be higher compared to that of base metal and 6PA and the high resistance towards corrosion and wear was attributed to the presence of MMO particles which were responsible for less reactivity of the surface.

Fotoohi *et al.* [33] fabricated hybrid surface composites from AA1050 reinforced with NiTiC powder through a 6-pass FSP procedure. The cylindrical tool was used in the fabrication of the hybrid surface composites with fixed traverse speed and rotational speed (40 mm/min and 1400 rpm, respectively). The typical increase in the number of FSP passes resulted in a homogeneous particle distribution and grain refinement. The microhardness analysis was found to be comparable similar to that reported in [30] and [32]. The UTS of 6PPA was found to be 2 times higher than that of base metal and 6PA (179 MPa, 84 MPa, and 90 MPa, respectively). The significant increase in tensile properties of hybrid surface composites is attributed to the microstructural phenomenon which includes Orowan's strengthening mechanism.

The cited literature in this section reveals that the reinforcement of nano-particles in AA1050 base metal yields almost common results.

2.1.2. Fabrication of Surface Composites using AA2xxx

The employment of a multi-pass FSP technique to produce surface composites has been extended to other series of aluminum alloys. The literature reveals that the AA2xxx series can also be used as the base metal in fabricating surface composites. Yang *et al.* [34] have utilized the multi-pass FSP technique to enhance the corrosion resistance of surface composites that were produced using the cold spraying technique. The 4-pass FSP procedure was conducted using a threaded cylindrical tool pin based on fixed tool rotational

speed and traverse speed (900 rpm and 50 mm/min, respectively). The hybrid surface composites fabricated through different FSP passes were studied comparatively to the cold sprayed (CS) material. The increase in the number of FSP passes resulted in a uniform distribution of reinforcement particles and grain refinement. The corrosion analysis revealed good corrosion resistance of composites fabricated using 1 and 2-pass FSP procedure compared to CS specimens and specimens produced from the 4-pass FSP procedure. The good corrosion behavior observed in specimens produced using low FSP passes was due to the reduced inter-splat spacing and dislocation density, surface re-oxidation of aluminum phase, the reduced volume fraction of S(S') phase, and redistribution of Al₂O₃ particles. In as much as high FSP pass results in grain refinement, however, there are other microstructural changes that may occur which affect the corrosion behavior of composites. This includes the reformation or coarsening of S(S') phases, high frequency of HAGBs, and high dislocation density.

Ghanbari *et al.* [35] have used the multi-pass FSP technique to fabricate surface composites from AA2024 which was reinforced with SiC nanoparticles. The fabrication of composites was based on a square tool pin profile. The 4-pass FSP procedure was conducted with a fixed tool rotational speed of 1000 rpm and a traverse speed of 25 mm/min. The specimens that were subjected to multi-pass FSP procedure were further heat-treated, hence the comparative analysis was conducted on heat-treated and untreated specimens. The increase in the number of FSP passes resulted in co-axial refined grains and the uniform distribution of SiC particles, and this was attributed to dynamic recrystallization. The microhardness of 2-pass and 4-pass FSP heat-treated specimens (2PH and 4PH) were relatively similar and a similar behavior was observed in untreated specimens (2P and 4P). However, the microhardness of 2PH and 4PH was 1.8 times higher than that of 2P and 4P. The enhancement in microhardness post-heat-treatment was attributed to the dissolution of S-phase precipitation during annealing and the reformation of finer S-phase precipitation during aging. The wear resistance of 2PH was 1.7 times higher than that of base metal, while 4PH exhibited wear resistance that was 1.2 times higher than that of the base metal. The wear resistance of 2P and 4P were found to be way lower than the base metal and this was attributed to the coarsening of S-phase precipitates. In as much as AA2xxx series can be used as the substrate in fabricating surface composites, the majority of works used AA2024, and not the other grades of AA2xxx series and there are limited works that have utilized the multi-pass FSP technique to produce AA2xxx series-based surface composites.

2.1.3. Fabrication of Surface Composites using AA5xxx

The literature has demonstrated that the AA5xxx series can be employed to produce surface composites with various reinforcements. Recent works have demonstrated that using multi-pass FSP plays a crucial role in various aspects of materials. This section reviews some works that have utilized

various AA5xxx series in fabricating surface composites through multi-pass FSP technique. Mirjavadi *et al.* [36] utilized a multi-pass FSP technique to reinforce ZrO₂ nanoparticles on the surface of AA5083 to produce surface nanocomposites. The threaded cylindrical tool pin profile was used to conduct an 8-pass FSP procedure based on fixed tool rotational speed and traverse speed (800 rpm and 50 mm/min, respectively). The increase in the number of FSP passes resulted in grain refinement and uniform distribution of reinforcement particles. The smaller equiaxed grains with a high level of HAGBs were achieved through an 8-pass FSP procedure. The composites produced from the 8-pass FSP procedure exhibited the highest tensile strength and microhardness compared to the base metal and other FSP passes. The percentage elongation was increasing with an increase in the number of FSP passes, however, all composite specimens were lower than that of the base metal. The wear resistance was found to be increasing with the increase in the number of FSP passes, with the highest FSP pass exhibiting higher wear resistance compared to the other passes and base metal. The improved mechanical properties were attributed to the microstructural modification posed by the iterated FSP procedure and the inclusion of reinforcement particles.

In one of the studies reported in the literature, multi-pass FSP was employed to fabricate hybrid surface composites from AA5056 and Zircon nanoparticles [37]. The tapered cylindrical tool pin profile was used in the fabrication of hybrid surface composites through a 4-pass FSP procedure. The tool rotational speed and traverse speed were fixed at 1000 rpm and 14 mm/min. The grain refinement was found to be improved with the increase in the number of FSP passes. The uniform dispersion of Zircon nanoparticles was observed in the composites fabricated through high FSP pass. The 4-pass composite specimen (4PP) exhibited a yield strength that was 2.7 times higher than that of the base metal. The UTS of 4PP was also found to be 1.5 higher than that of the base metal. However, the 3PP specimen exhibited a higher percentage elongation compared to the base metal and other specimens (1.4 times higher than BM). The improved yield and tensile strengths were attributed to the strain hardening and density value of the specimen. The drop in percentage elongation on the 4PP specimen was attributed to the dramatic change in dislocation due to the high number of FSP passes. The microhardness of the 4PP was higher than that of the base metal (90 HV to 69 HV). The microstructural analysis for 4PP revealed that this specimen had finer grains which were coupled with a high density of dislocations and high level of HAGBs. This microstructural phenomenon has contributed to the drop in corrosion resistance of this specimen.

Sharifitabar *et al.* [38] fabricated surface composites from AA5056 and Al₂O₃ nanoparticles through the use of a multi-pass FSP technique. The cylindrical tool pin profile was used in executing a 4-pass FSP procedure. The optimized FSP parameters (rotational speed-1600 rpm; traverse speed-16 mm/min; tilt angle-5°) were used in conducting the FSP procedure. The mechanical properties of the fabricated hybrid surface composites were studied comparatively with the

friction stir processed AA5056 without reinforcement particles. The grains in both cases (with and without reinforcements) were reduced linearly with the increase in the number of FSP passes, however, the specimens with reinforcement were dominated by finer grains (ranging between 0.97 μm and 5.5 μm). There was homogeneity in Al₂O₃ particles distribution observed in the composites produced with higher FSP passes. It was further observed that the composite specimens produced from high FSP passes were dominated by high dislocation density and high level of HAGBs. The yield strength and tensile strength were both increased with an increase in the number of FSP passes for the FSP conducted with and without reinforcement. However, the composites' specimens exhibited tensile and yield strengths that were higher than the specimens processed without reinforcement. This domination in tensile properties was attributed to the highly refined grains and the high level of HAGBs. The percentage elongation showed an increasing trend from 1-pass FSP until 3-pass FSP for composites and processed specimens without reinforcements, and the decline in percentage elongation followed beyond 3-pass FSP. This behavior was attributed to an increase in dislocation density associated with higher FSP passes.

Yang *et al.* [39] have utilized a multi-pass FSP technique to fabricate surface composites from AA5083 and AlCoCrFeNi high-entropy alloy particles (HEA). The threaded cylindrical tool profile was used to conduct a 5-pass submerged FSP procedure. The multi-pass SFSP was conducted based on fixed tool rotational speed and traverse speed (1400 rpm and 40 mm/min, respectively). The major difference in this study from the previously mentioned studies is that the fabrication of surface composites was performed underwater. The specimens processed with and without the inclusion of reinforcement particles were studied comparatively. The microstructural analysis revealed the LAGBs were higher compared to HAGBs in the base metal. However, the processed specimens revealed that about 62% of LAGBs were transformed into HAGBs post FSP. The inclusion of reinforcement particles influenced the further transformation of LAGBs, hence higher HAGBs (65%) in composites compared to processed specimens. The UTS and yield strength of the composites were 1.2 and 1.3 times higher than those of the processed specimen and base metal, respectively. However, the percentage elongation of the composites was 26% and 16% lower than that of the processed specimens and base metal. The enhanced tensile properties were attributed to the refined grains associated with composites, while the drop in percentage elongation was defined as a generic phenomenon for aluminum matrix composites reinforced with ceramic particles

There are more other studies where AA5xxx series was used as the base metal or substrate and the majority of those studies showed that various properties of composites fabricated using multi-pass FSP technique improve with an increase in the number of FSP passes [40–49].

2.1.4. Fabrication of Surface Composites using AA6xxx

The utilization of the AA6xxx series in the fabrication of hybrid surface composites through a multi-pass FSP technique is reviewed. The tribological properties of AA6082 were improved through the reinforcement of SiC particles via the multi-pass FSP technique [50]. The tool with a square pin profile was used in conducting a multi-pass FSP procedure. The 3-pass FSP procedure was conducted based on a fixed tool rotational speed of 1400 rpm and a traverse speed of 40 mm/min. The severe plastic deformation coupled with SiC particles were found to be responsible for the grain reduction at the stir zone. The reduction in grain size was found to be dependent on the number of FSP passes. The homogeneous dispersion of reinforcement particles was observed in composites produced from high FSP passes. The microhardness of the composites was found to be increasing with the increase in FSP passes with the highest hardness value (154 HV) corresponding to the composites produced through the 3-pass FSP procedure. The increase in microhardness is attributed to the homogeneous dispersion of SiC particles and grain refinement. The composites produced using the 3-pass FSP procedure exhibited UTS that is 1.3 times higher than the base metal and this is attributed to the strengthening mechanism that is always associated with SiC reinforcement particles. This SiC strengthening mechanism always comes with the compromise in ductility, hence the composites with high UTS exhibited low percentage elongation. The surface analysis revealed that the surface roughness of the composites decreased with an increase in the number of FSP passes. The decrease in surface roughness was attributed to the improvement of SiC particles mixing in the aluminum matrix. The wear resistance of composites produced from high FSP pass was found to be 1.5 times higher than the base metal and this was attributed to the homogeneous dispersion of SiC particles.

Nazari *et al.* [51] have investigated the mechanical properties and wear behavior of hybrid surface composites produced from AA6061 reinforced with TiB₂ and graphene particles via multi-pass FSP technique. The composites were fabricated using the tool with a prismatic pin profile. The fixed traverse speed and tool rotational speed were utilized in conducting the 4-pass FSP procedure. Different concentrations of reinforcements were used in fabricating the composites. The microstructural analysis revealed a uniform distribution of reinforcement particles was observed in composites fabricated at a high number of FSP passes. The grain refinement reported in other works [39] – [50] was also observed in this investigation. The microhardness of the composites reinforced with 20 wt% of TiB particles and 1 wt% graphene particles was found to be 1.4 times higher than that of the base metal, while other combinations exhibited microhardness that was lower than this. The composite that was reinforced with 20 wt% of TiB and 2 wt% of graphene exhibited UTS and yield strengths that were 1.8 and 3 times higher than those of the base metal. The other composites reinforced with other concentrations exhibited tensile

properties that were lower than this composite. The composites reinforced with 1 wt% of graphene and the processed specimen without reinforcement exhibited a percentage elongation that was 1.2 higher than that of the base metal. The phenomenon behind the improved tensile properties is similar to that explained in [38] – [39]. The composites reinforced with 20 wt% of TiB and 1 wt% of graphene exhibited high wear resistance compared to other specimens, and the improved wear resistance of these composites was attributed to the presence of graphene reinforcement which acted as the lubricant agent.

Sharma *et al.* [52] have investigated the reinforcement distribution mechanism of hybrid surface composites produced from AA6061 and graphene nanoplatelets via the multi-pass FSP technique. The cylindrical tool pin profile was used in the fabrication of hybrid surface composites. The tool rotational speed and traverse speed were fixed at 1400 rpm and 40 mm/min, respectively. The influence of the impregnation method towards the properties of the composites was investigated, hence reinforcements were filled in multiple-micro channels (MMCRF) and single-micro channel (SCRF). The peak temperature recorded during the fabrication of composites with reinforcements filled with MMCRF was higher compared to those composites produced when the SCRF method was used. The uniform distribution of graphene nanoplatelets (GNP) was observed on the specimens produced through the use of the MMCRF strategy and no defects were detected on the surface of the fabricated composites. There was no trace of brittle intermetallics observed at the Al matrix and GNP interface. The composites produced through the SCRF strategy showed the trace of GNP agglomeration and clustering and this was attributed to the low heat input required for homogeneous particle distribution in the Al matrix. The non-homogeneous dispersion of GNP in composites produced through SCRF resulted in increased plastic strain and high residual stresses. The UTS of the composite produced through the MMCRF strategy was 1.3 and 1.04 times higher than the composites produced through SCRF strategy and processed base metal, respectively. However, the yield strength of the composite produced through the SCRF method was 1.1 and 1.3 times higher compared to the composites produced through the MMCRF strategy and the processed base metal, respectively. The percentage elongation of the processed base metal was 6.4 and 1.8 times higher than the composites produced through SCRF and MMCRF strategies, respectively. The composites produced through MMCRF exhibited a 115% increase in hardness compared to processed base metals while 31% was the recorded increase in hardness of the composite produced through the SCRF method with processed base metals.

Du *et al.* [53] have employed 3-pass FSP to produce surface composites from AA6061 reinforced with Al₂O₃ particles and carbon nanotubes (CNT). The threaded conical tool pin profile with three flats was used in the fabrication of hybrid surface composites. The tool rotational speed and traverse speed were fixed at 1200 rpm and 3 mm/s, respectively. The dispersion of CNT throughout the Al matrix was observed in

the composites produced through a high number of FSP passes. The composites produced with the reinforcement of both Al_2O_3 and CNT exhibited higher microhardness value compared to those processed base metals (1.6 times higher than the processed base metal). The UTS and yield strength for composites produced with the reinforcement of both Al_2O_3 and CNT was 1.2 and 1.7 times higher than the processed base metal. However, the percentage elongation of the processed base metal was 4.5 times higher than the composites produced with the reinforcement of both Al_2O_3 and CNT.

More works have reported on the impact of fabricating surface composites using multi-pass technology [54] – [57].

2.1.5. Fabrication of Surface Composites using AA7xxx

Studies have demonstrated that AA7xxx can also be used for the fabrication of surface composites. Netto *et al.* [58] have reinforced NiTi/Al particles into the AA7075 plate with 8-pass FSP to produce a hybrid surface composite. The threaded conical tool pin profile was used in the fabrication of hybrid surface composites. The tool rotational speed and traverse speed were fixed at 400 rpm and 100 mm/min, respectively. The filling of reinforcement particles was based on two strategies, i.e., groove and multi-hole strategies. The comparative analysis was performed on a 4-pass and 8-pass FSP procedure taking into account the filling strategy. The homogeneous distribution of NiTi particles was observed in 4-pass and 8-pass FSP procedures with no traces of particle clustering for the composites produced using the groove filling strategy. The inhomogeneous distribution of NiTi particles was observed in the composites produced through a multi-hole filling strategy. The tensile strength of the composite produced through the groove and multi-hole filling strategies was relatively similar. However, the percentage elongation of composites produced via the groove strategy was higher compared to composites produced through multi-hole strategy. The difference in percentage elongation is attributed to the homogenous distribution of NiTi particles and grain size reduction.

Rana *et al.* [59] have investigated the wear behavior of AA7075/ B_4C composites fabricated with the multi-pass FSP technique. The hybrid surface composites were fabricated using a tapered cylindrical tool pin profile based on 545 rpm rotational speed and varying traverse speed (50, 78, and 120 mm/min). The B_4C particle agglomeration was observed in specimens that were produced using low traverse, while the homogeneous dispersion of reinforcement particles was observed from particles produced with high traverse speed. The microstructural defects were also observed from specimens produced through low traverse speed and diminished in specimens produced through high traverse speed. The grain refinement due to intense plastic deformation and frictional heat was achieved. The microhardness and wear resistance of the composites declined with an increase in traverse and this was attributed to insufficient mixing time due to increased traverse speed.

Garcia-Vazquez *et al.* [60] have investigated the influence of multi-pass FSP on the properties of AA7075/TiC composites. The hybrid surface composites were fabricated using a tapered cylindrical tool pin profile based on 1000 rpm rotational speed and traverse speed of 300 mm/min. The sealed and unsealed groove filling strategies were used in conjunction with two FSP passes either in the same or different directions. The surface of all specimens revealed no surface cracks or defects. The particle agglomeration was observed on the retreating side of the specimens that were prepared with an unsealed grooves and 2-pass FSP rotating in the same direction. The uniform distribution of particles and refinement of grains was observed in specimens prepared by sealed groove and 2-pass FSP performed in different rotating directions. The microhardness and wear resistance were higher for the specimens prepared with sealed grooves and 2-pass rotating in different directions. It was also observed that the wear resistance of composites dropped compared to the base metal and this was attributed to a low concentration of reinforcement.

Ande *et al.* [61] have investigated the effect of the number of FSP passes on the wear behavior and microhardness of AA7075/SiC composites. The hybrid surface composites were fabricated using a tapered cylindrical tool pin profile based on 1200 and 1400 rpm rotational speed and traverse speed of 30 and 40 mm/min. It was discovered that the variation of traverse speed had an insignificant contribution towards the microstructural arrangement. However, the increase in rotational speed played a role in a homogeneous distribution of particles and the refinement of grains. The specimens produced (at 3-pass FSP) using 1200 and 1400 rpm at constant traverse speed (30 mm/min) exhibited microhardness that was 1.7 and 2.1 times higher than that of the base metal. The specimens produced at high 1200 rpm and 40 mm/min (3-pass FSP) exhibited excellent wear resistance compared to specimens produced from other combinations of parameters, and this was attributed to the refined grains and homogeneous dispersion of the reinforcement particles. The influence of using multi-pass FSP to produce surface composite from AA7xxx majorly lies in the particle distribution which has an impact on various properties of the fabricated surface composites.

2.1.6. Summary

The literature surveyed reveals that the multi-pass FSP technique has been used to fabricate surface composites from various aluminum alloys. It is observed that the multi-pass FSP technique assists with the enhancement of reinforcement particle distribution irrespective of aluminum grade [62–71]. It has become apparent that the reinforcement particle distribution homogeneity assists with the enhancement of microhardness and tensile properties. Figure 4 shows the comparison between the ultimate strength (UTS) of base metal used in composite fabrication and the fabricated composites. The UTS of composites produced through multi-pass FSP is consistently higher than the base metal used

in composites. The enhanced UTS is a result of grain refinement and uniform distribution of reinforcement particles. The improvement of UTS comes from the loss of percentage elongation for most composites (see Figure 5). The hardness of composites produced through multi-pass FSP is consistently higher than the base metal (see Figure 6). The enhanced composites' hardness is attributed to the refined grains and the uniform distribution of reinforcement particles.

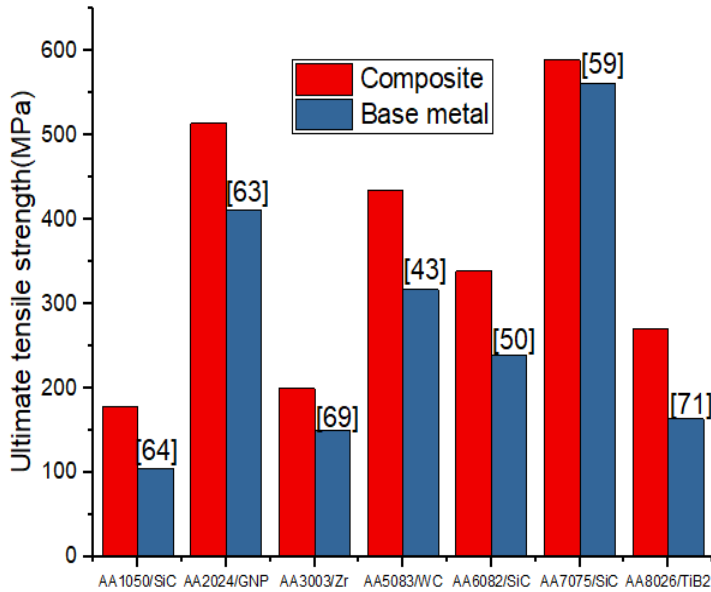


Figure 4. Ultimate tensile strength of base metal and surface composites fabricated via multi-pass FSP.

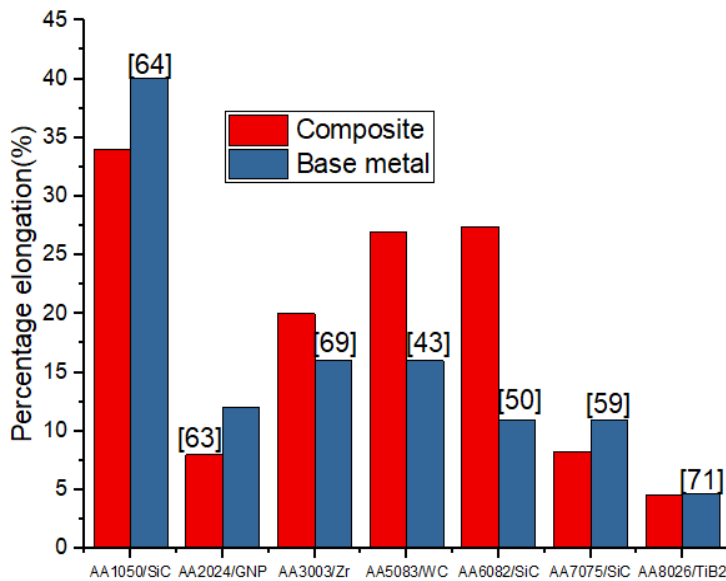


Figure 5. Percentage elongation of base metal and surface composites fabricated via multi-pass FSP.

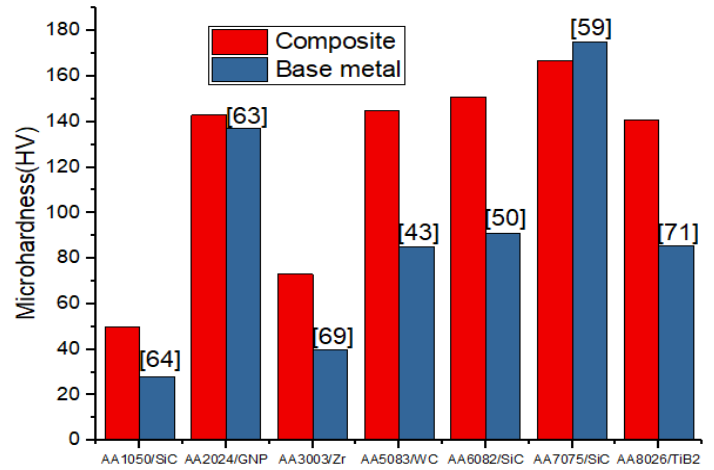


Figure 6. Ultimate tensile strength of base metal and surface composites fabricated via multi-pass FSP.

2.2. Microstructural Modification of Aluminum Alloys using Multi-Pass FSP Technique

The literature has shown that multi-pass FSP technique can be utilized in modifying materials without incorporating reinforcements. The employment of the multi-pass FSP technique to modify the microstructure of various alloys of aluminum is discussed in detail in this section. The schematic diagram depicting the FSP of a single plate is shown in Figure 7.

El-Rayes and El-Danef [72] have employed the multi-pass FSP technique to modify the microstructure of AA6082 using constant rotational speed (850 rpm) and varying traverse speed (90, 140, 224 mm/min). The concentric square pin profile was utilized in carrying out the 3-pass FSP procedure. The increase in traverse speed and number of FSP passes resulted in a notable increase in the high level of HAGBs. The increase in the number of FSP passes and traverse speed resulted in an increase in grain size. However, the grain coarsening was found to be mostly affected by the number of FSP passes than the increase in traverse speed. The increase in the number of FSP passes resulted in the increment in second-phase particle density, whereas the increase in traverse speed resulted in a reduction of particle size. The increase in the number of passes resulted in the decline in microhardness at the stir zone and this was attributed to the grain coarsening. However, increasing the traverse speed resulted in the linear increase in microhardness and this behavior was attributed to the nucleation sites of new precipitates due to higher stirring of the plasticized material. The increase in the number of FSP passes resulted in grain growth and the dissolution of β'' precipitates (due to high heat exposure), hence UTS declined with an increase in the number of FSP passes. However, the increase in traverse speed resulted in the refinement of particle size and this contributed to the enhancement of UTS at the stir zone. Nakata et al. [73] have employed a multi-pass FSP technique to modify the microstructure of die-casting aluminum alloy (DC12). The columnar-shape with a screw pin profile was utilized in conducting a multi-pass FSP procedure. The

processing parameters were fixed at 1250 rpm (rotational speed) and 500 mm/min (traverse speed). The mechanical properties of the specimens sampled parallel to the processing direction were studied comparatively to those sampled perpendicular to the processing direction. The hardness of the processed specimens was 20 HV higher than the base metal and this hardness increase was attributed to the grain refinement and the redistribution of Si particles post multi-pass FSP procedure. The tensile strength of the processed specimens sampled parallel and perpendicular to the processing direction was 1.7 times higher than the base metal. Thus there was no significant difference between the specimens sampled from different directions of the processed plate. The significant increase in UTS for the processed specimens was attributed to the grain refinement and redistribution and refinement of Si particles due to dynamic recrystallization.

Alfadhlah *et al.* [74] have employed multi-pass FSP to modify the microstructure of AA6063. The cylindrical tool pin profile was used in performing a 3-pass FSP procedure. The processing parameters were fixed at 600 rpm and 145 mm/min (rotational speed and traverse speed, respectively). The typical grain refinement was observed at the stir zone and the very same zone was dominated by a high level of HAGBs due to dynamic recrystallization. The grain growth was observed in specimens that were subjected to heat treatment post multi-pass FSP procedure. However, the bimodal grain growth was also observed for specimens that were heat treated. There was a significant decline in UTS for the processed specimens, while a regain in UTS was observed from specimens that were subjected to heat treatment. The decline in UTS for processed specimens was attributed to the dissolution of very fine hardening precipitates due to high heat input during processing. The regain in UTS was attributed to the reprecipitation of hardening precipitates due to artificial aging. The microhardness followed the same trend observed in UTS and the reasoning behind the behavior was the same. Chen *et al.* [75] have subjected A7B04 to a multi-pass FSP technique to analyze its impact on the microstructure and mechanical properties. The M5 cylindrical tool pin profile was used in performing a 3-pass FSP procedure. The processing parameters were fixed at 400 rpm and 200 mm/min (rotational speed and traverse speed, respectively). The severe plastic deformation experienced in the stir zone resulted in equiaxed refined grains and the variation in grain size due to variation in the number of FSP passes was ignored due to insignificance. The processed specimens were all dominated by a relatively similar fraction of HAGBs. The microhardness of the processed specimens increased with an increase in the number of FSP passes, and this increase was attributed to the grain refinement. The specimens subjected to 1-pass FSP exhibited UTS and yield strength that was 1.5 and 2 times higher than the base metal, respectively. However, a notable decline in UTS and yield strength was observed for the specimens produced at a higher number of FSP passes.

The impact of employing a multi-pass FSP technique on hypo-eutectic Al-Si was reported from the work conducted by

Meenia *et al.* [76]. The threaded tapered cylindrical tool pin profile was used in performing the 3-pass FSP procedure. The processing parameters were fixed at 800 rpm and 120 mm/min (rotational speed and traverse speed, respectively). The multi-pass FSP technique was employed on solution-treated specimens and untreated materials. The increase in the number of FSP passes for both conditions of the base metal resulted in a uniform distribution and fragmentation of Si particles. There was also a notable decrease in porosity with an increase in the number of FSP passes for both conditions of the base metal. The mechanical properties of the untreated base metal were studied comparatively with the treated specimens and there was a notable increase in the mechanical properties of treated specimens compared to untreated specimens. The improvement in mechanical properties was attributed to the dissolution of the acicular shape of Si particles post solution treatment. The increase in the number of FSP passes for untreated base metal yielded the refined grains, reduced porosity, volume fraction, and homogeneous dispersion of Si particles, hence a linear increase in microhardness with the number of FSP passes. However, the decline in microhardness was observed in the processed treated specimens and this decline was attributed to over-aging imposed by the FSP process, which resulted in the coarsening of Mg₂Si particles. The UTS of 3-pass FSP treated and untreated specimens were 1.7 and 1.3 times higher than that of the base metal. The yield strengths of 3-pass FSP treated and untreated specimens were also 1.5 and 1.2 times higher than that of the base metal. The percentage elongation of 3-pass FSP treated and untreated specimens were 5.1 and 7.6 times higher than that of the base metal. The improved tensile properties were attributed to the significant reduction in porosity volume fraction.

Chen *et al.* [77] have employed a multi-pass FSP technique to modify the microstructure of AA5083. The threaded tapered cylindrical tool pin profile was used in performing the 3-pass FSP procedure. The performance of multi-pass FSP was based on a fixed traverse speed (360 mm/min) and two varying rotational speeds (600 and 1200 rpm). The increase in the number of FSP passes resulted in the refinement of stir zone grains and more transformation of LAGBs to HAGBs. However, the increase in rotational speed resulted in the coarsening of grains in the stir zone with an insignificant impact on grain boundary transformation. The yield strength of the specimens produced at a low and high rotational speed with a high number of FSP passes (3-pass) was 14.8% and 21.3% less than that of the base metal. The UTS of specimens produced at a low and high rotational speed with a high number of FSP passes (3-pass) was 10.1% and 5.8% less than that of the base metal. However, the percentage elongation of specimens produced at a low and high rotational speed with a high number of FSP passes was 1.5 and 1.7 times higher than that of the base metal. The stir zone of the processed specimens (irrespective of several FSP passes) exhibited a reduced microhardness compared to the base metal and this reduction was attributed to the annealing softening and recrystallization. However, the increase in the number of FSP passes assisted with the inhibition of the expansion of

abnormal grain growth and these results are in agreement with those achieved by Jana *et al.* [78].

Singh *et al.* [79] have analyzed the impact of the multi-pass FSP technique on the properties of Al-Si hypoeutectic A356 alloy. The tapered cylindrical tool pin profile was used in performing a 3-pass FSP procedure. The performance of multi-pass FSP was based on a fixed traverse speed (120 mm/min) and rotational speeds (800 rpm). The coarse Si particles were refined and homogeneously dispersed in α -aluminum phase post multi-pass FSP procedure. The porosity volume fraction decreased significantly with an increase in the number of FSP passes. The UTS and yield strength of the specimens processed using the 3-pass FSP procedure were 1.3 and 1.2 times higher than those of the base metal, respectively. The percentage elongation of specimens processed with the 3-pass FSP procedure was 7.6 times higher than that of the base metal. The specimens subjected to 3-pass FSP exhibited excellent metallic wear resistance compared to other specimens, while 2-pass specimens showed good abrasive wear resistance. The 1-pass and 2-pass FSP specimens exhibited low drilling force and surface roughness, while higher drilling force and surface roughness was observed in specimens produced from the 3-pass FSP procedure. The enhanced mechanical and tribological properties were attributed to the grain refinement and homogeneous distribution of strengthening particles.

The utilization of a multi-pass FSP technique on a simple aluminum plate (no special treatment) yields different results. The response of the specimens subjected to the multi-pass FSP procedure depends on the nature of the base metal. However, the majority of works agreed that the increase in the number of FSP passes results in grain refinement. However, grain refinement does not necessarily translate to improved mechanical properties [80] – [86].

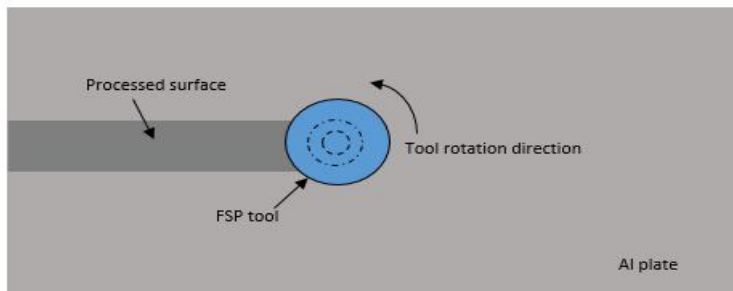


Figure 7. Top view schematic diagram for multi-pass FSP performance

2.3. Microstructural Modification of Similar/Dissimilar Aluminum Alloy Welded Joints using Multi-Pass FSP Technique

Multi-pass friction stir processing is still categorized as an emerging technique for material performance enhancement. The previous sections have demonstrated the progress made in utilizing this technique for various purposes. The top view schematic diagram depicting the multi-pass FSP setup for welded joints is shown in Figure 8. This section reviews the use of the multi-pass FSP technique to modify the microstructure of welded joints.

Mabuwa and Msomi [87] have investigated the influence of multi-pass FSP on the fatigue strength of AA8011/AA6082. The rectangular threaded tool pin profile was used in performing a 4-pass FSP procedure. The performance of multi-pass FSP was based on a fixed traverse speed (45 mm/min) and rotational speeds (1100 rpm). The friction stir welding technique was used to produce an AA8011/AA6082 dissimilar joint, which was then subjected to the four-pass FSP technique. The grain refinement pattern revealed that the refinement of grains was not depending on the multi-pass FSP technique but also the material positioning during processing. The UTS of the 4-pass FSP specimens produced when AA8011 on the advancing side was 69% less than that of AA6082 base metal but matched that of AA8011 base metal. The UTS of the 4-pass FSP specimens produced when AA6082 on the advancing side was 70.4% less than that of AA6082 base metal and slightly less than that of AA8011 base metal. The percentage elongation of the 4-pass FSP specimens produced when AA8011 on the advancing side was 6.5% less than that of AA6082 base metal and 41% less than that of AA8011 base metal. There was an insignificant change in percentage elongation due to material positioning change. The fatigue life of joints processed with AA6082 on the advancing side was found to be higher compared to AA6082 on the retreating side. The increase in the number of FSP passes increased the fatigue life of the joint. A recent similar study was also performed by Mabuwa and Msomi [88]. However, the 4-pass technique was performed under cold water. The increase in the number of FSP passes resulted in the refined equiaxed grains dominating the stir zone of the welded joint. It was also observed that the mechanical properties of the processed joint were not uniform along the joint. The specimens sampled from the center towards the end of the joint exhibited higher mechanical properties compared to those sampled from the start of the joint. The difference in mechanical along the joint was attributed to non-homogeneous grain size which was affected by the heat input. The specimens sampled from the middle and the end of the joint exhibited microhardness that was 2.4 times higher than that of AA8011 base metal but lower than that of AA6082 base metal. It was also reported that all processed specimens fractured in the heat-affected zone of the base metal with lower tensile strength.

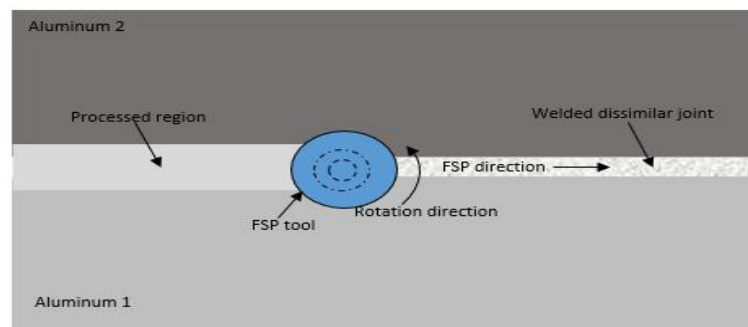


Figure 8. Top view schematic diagram for multi-pass FSP performed on dissimilar welded joint.

The employment of the multi-pass FSP technique on joints is still a new area, hence the limited work available. The included works under this section are the only available works that suit this section, hence no further work is included.

3. CONCLUDING REMARKS

This work has attempted to track the status and progress of the employment of multi-pass FSP technology. The multi-pass FSP technique is a new and emerging technology that has been tested for various applications. This includes the employment of this technique in producing composites, materials, and surfaces. However, it has been observed that the majority of works focused on utilizing the multi-pass FSP technique to produce composites than to utilize it on other conditions like single plates and welded joints. The literature gives a clear picture of the benefit of using multi-pass FSP in fabricating hybrid composites. However, it is not quite clear if what is the impact of subjecting single plate surfaces to the multi-pass FSP technique as each material responds differently. There is only one recent literature available on the employment of multi-pass FSP to the welded joint. The recent literature also focused on the friction stir welded dissimilar joint and there is no available literature that reports about the employment of this technique on joints welded using other welding techniques. There is further no work that report about employing the technique on various dissimilar joints. This then opens a gap to pursue the multi-pass friction stir processing on other types of welded joints. Future works could consider the reinforcement of nanoparticles into the welded joints as the method of enhancing the joints.

ACKNOWLEDGEMENT

The authors would like to thank National Research Foundation for financial assistance.

REFERENCES

1. V. Msomi and N. Mbana. **Mechanical properties of friction stir welded AA1050-H14 and AA5083-H111 joint: Sampling aspect.** *Metals*, Vol. 10, no. 2, 2020.
2. H.J. Liu, H. Fujii, M. Maeda M, and K. Nogi. **Mechanical properties of friction stir welded joints of 1050 – H24 aluminium alloy.** *Science and Technology Welding and Joining*, Vol. 8, no. 6, pp. 450-454, 2003.
3. M. Ilangoan, S.R. Boopathy, and V. Balasubramanian. **Microstructure and tensile properties of friction stir welded dissimilar AA6061-AA5086 aluminium alloy joints.** *Transactions of Nonferrous Metals Society of China*, Vol. 25, no. 4, pp. 1080-1090, 2015.
4. M. Maurya, S. Kumar, and V. Bajpai. **Assessment of the mechanical properties of aluminium metal matrix composite: A review.** *Journal of Reinforced Plastics and Composites*, Vol. 38, no. 6, pp. 267-298, 2018
5. P. Sampath, V.K. Parangodath, K.R. Udupa, and U.B. Kuruveri. **Fabrication of Friction Stir Processed Al-Ni Particulate Composite and Its Impression Creep Behaviour.** *Journal of Composites*, Vol. 2015, 428630, 2015
6. G. Çam and M. Koçak. **Progress in joining of advanced materials.** *Interantaional Materials Reviews*, Vol. 43, no. 1, pp. 1-44, 1998
7. J.E. Gould, T.J. Lienert, and Z. Feng. **Recent Developments in Friction Stir Welding.** *Journal of Material Science and Manufacturing*, Vol. 107, pp. 1093-1100, 1998.
8. S. Mabuwa and V. Msomi. **Comparative analysis between normal and submerged friction stir processed friction stir welded dissimilar aluminium alloy joints.** *Journal of Materials Research and Technology*, Vol.9, no. 5, pp. 9632-9644, 2020.
9. V. Msomi and S. Mabuwa. **Analysis of material positioning towards microstructure of the friction stir processed AA1050/AA6082 dissimilar joint.** *Advances in Industrial Manufacturing and Engineering*, Vol. 1, 100002, 2020.
10. K. Palani, C. Elanchezhian, V.B. Ramnath, G.B. Bhaskar, and E. Naveen. **Effect of pin profile and rotational speed on microstructure and tensile strength of dissimilar AA8011, AA01-T6 friction stir welded aluminum alloys.** *Materials Today: Proceedings*, Vol. 5, no. 11, pp.24515-24524, 2018.
11. M.K. Gupta. **Friction stir process: a green fabrication technique for surface composites—a review paper.** *SN Applied Science*, Vol. 2, no. 4, ID 532, 2020.
12. Mabuwa S, Msomi V. **Effect of Friction Stir Processing on Gas Tungsten Arc-Welded and Friction Stir-Welded 5083-H111 Aluminium Alloy Joints.** *Advanced Material Science and Engineering*, Vol. 2019, ID 3510236, 2019.
13. A. Kurt, I. Uygur, and E. Cete. **Surface modification of aluminium by friction stir processing.** *Journal of Material Processing and Technology*, Vol.211, no. 3, pp. 313-317, 2011.
14. H. Kumar, R. Prasad, P. Kumar, S.P. Tewari, and J.K. Singh. **Mechanical and tribological characterization of industrial wastes reinforced aluminum alloy composites fabricated via friction stir processing.** *Journal of Alloys Compounds*, Vol. 831, ID154832, 2020.
15. J.J. Pang, F.C. Liu, J. Liu, M.J. Tan, and D.J. Blackwood. **Friction stir processing of aluminium alloy AA7075: Microstructure, surface chemistry and corrosion resistance.** *Corrosion Science*, Vol. 106, pp. 217-228, 2016.
16. D.C. Hofmann and K.S. Vecchio. **Submerged friction stir processing (SFSP): An improved method for creating ultra-fine-grained bulk materials.** *Material Science and Engineering A*, Vol.402, no. 1-2, pp. 234-241, 2005.
17. R.S. Mishra, Z.Y. Ma, and I. Charit. **Friction stir processing: a novel technique for fabrication of surface composite.** *Material Science and Engineering A*, Vol. 341, no. 1, pp. 307-310, 2003.
18. H. Mehdi and R.S. Mishra. **Effect of Friction Stir Processing on Microstructure and Mechanical Properties**

of **TIG Welded Joint of AA6061 and AA7075**. *Metallography and Microstructural Analysis*, Vol. 9, no. 3, pp. 403-418, 2020.

19. R. Abrahams, J. Mikhail, P. Fasihi. **Effect of friction stir process parameters on the mechanical properties of 5005-H34 and 7075-T651 aluminium alloys**. *Material Science and Engineering A*, Vol. 751, pp. 363-373, 2019.

20. P. Nelaturu, S. Jana, R.S. Mishra, G. Grant, and B.E. Carlson. **Influence of friction stir processing on the room temperature fatigue cracking mechanisms of A356 aluminum alloy**. *Material Science and Engineering A*, Vol. 716, pp. 165-178, 2018.

21. W. Yang, H. Ding, Y. Mu, J. Li, W. Zhang. **Achieving high strength and ductility in double-sided friction stir processing 7050-T7451 aluminum alloy**. *Material Science and Engineering A*, Vol.707, pp. 193-198, 2017.

22. V.V. Patel, V.J. Badheka, U. Patel, S. Patel, S. Zala, K. Badheka. **Experimental Investigation on Hybrid Friction Stir Processing using compressed air in Aluminum 7075 alloy**. *Materials Today: Proceedings*, Vol. 4, no. 9, pp. 10025-10029, 2017.

23. M.L. Santella, T. Engstrom, D. Storjohann, T.Y. Pan. **Effects of friction stir processing on mechanical properties of the cast aluminum alloys A319 and A356**. *Script Materialia*, Vol. 53, no. 3, pp. 201-206, 2005

24. D. Yadav, R. Bauri. **Effect of friction stir processing on microstructure and mechanical properties of aluminium**. *Material Science and Engineering A*, Vol.539, pp. 85-92, 2012.

25. Q. Qin, H. Zhao, J. Li, J. Zhang, X. Su. **Microstructure and mechanical properties of friction stir processed Al-Mg2Si alloys**. *Transactions of Nonferrous Metals Society of China*, Vol. 30, no. 9, pp. 2355-2368, 2020.

26. F. Liu, Y. Ji, Z. Sun, J. Liu, Y. Bai, Z. Shen. **Enhancing corrosion resistance and mechanical properties of AZ31 magnesium alloy by friction stir processing with the same speed ratio**. *Journal of Alloys and Compounds*, Vol. 829, ID 154452, 2020.

27. C.Y. Ma, L. Zhou, R.X. Zhang, D.G. Li, F.Y. Shu, X.G. Song. **Enhancement in mechanical properties and corrosion resistance of 2507 duplex stainless steel via friction stir processing**. *Journal of Materials Research and Technology*, Vol. 9, no. 4, pp. 8296-8305, 2020.

28. S.R. Sharma, Z.Y. Ma, R.S. Mishra. **Effect of friction stir processing on fatigue behavior of A356 alloy**. *Script Materialia*, Vol.51, no. 3, pp. 237-241, 2004.

29. S. Jana, R.S. Mishra, J.B. Baumann, G. Grant. **Effect of stress ratio on the fatigue behavior of a friction stir processed cast Al-Si-Mg alloy**. *Script Materialia*, Vol.61, no. 10, pp. 992-995, 2009.

30. M. Alishavandi, M. Ebadi, S. Alishavandi, A.H. Kokabi. **Microstructural and mechanical characteristics of AA1050/mischmetal oxide in-situ hybrid surface nanocomposite by multi-pass friction stir processing**. *Surface Coatings Technology*, Vol. 388, ID 125488, 2020.

31. G. Azimi-Roeeen, S.F. Kashani-Bozorg, M. Nosko, L. Orovicik, S. Lotfian. **Effect of multi-pass friction stir**

processing on textural evolution and grain boundary structure of Al-Fe3O4 system. *Journal of Materials Research Technology*, Vol. 9, no. 1, pp. 1070-1086, 2020.

32. M. Alishavandi, R.M.A. Kholari, M. Ebadi, S. Alishavandi, A.H. Kokabi. **Corrosion-wear behavior of AA1050/mischmetal oxides surface nanocomposite fabricated by friction stir processing**. *Journal of Alloys Compounds*, Vol.832, ID 153964, 2020.

33. H. Fotoohi, B. Lotfi, Z. Sadeghian, J. Byeon. **Microstructural characterization and properties of in situ Al-Al3Ni/TiC hybrid composite fabricated by friction stir processing using reactive powder**. *Material Characterization*, Vol.149, pp. 124-132, 2019.

34. K. Yang, W. Li, Y. Xu, X. Yang. **Using friction stir processing to augment corrosion resistance of cold sprayed AA2024/Al2O3 composite coatings**. *Journal of Alloys and Compounds*, Vol. 774, pp. 1223-1232, 2019.

35. D. Ghanbari, K.M. Asgarani, K. Amini, F. Gharavi. **Influence of heat treatment on mechanical properties and microstructure of the Al2024/SiC composite produced by multi-pass friction stir processing**. *Measurement*, Vol. 104, pp. 151-158, 2017.

36. S.S. Mirjavadi, M. Alipour, A.M.S. Hamouda, A. Matin, S. Kord, B.M. Afshari. **Effect of multi-pass friction stir processing on the microstructure, mechanical and wear properties of AA5083/ZrO2 nanocomposites**. *Journal of Alloys and Compounds*, Vol. 726, pp. 1262-1273, 2017.

37. M. Rahsepar, H. Jarahimoghadam. **The influence of multipass friction stir processing on the corrosion behavior and mechanical properties of zircon-reinforced Al metal matrix composites**. *Material Science and Engineering A*, Vol. 671, pp. 214-220, 2016.

38. M. Sharifitabar, A. Sarani, S. Khorshahian, S.M. Afarani. **Fabrication of 5052Al/Al2O3 nanoceramic particle reinforced composite via friction stir processing route**. *Materials and Design*, Vol.32, no. 8, pp. 4164-4172, 2011.

39. X. Yang, P. Dong, Z. Yan, B. Cheng, X. Zhai, H. Chen. **AlCoCrFeNi high-entropy alloy particle reinforced 5083Al matrix composites with fine grain structure fabricated by submerged friction stir processing**. *Journal of Alloys and Compounds*, Vol. 836, ID 155411, 2020.

40. S. Sahraeinejad, H. Izadi, M. Haghshenas, A.P. Gerlich. **Fabrication of metal matrix composites by friction stir processing with different Particles and processing parameters**. *Material Science and Engineering A*, Vol.626, pp. 505-513, 2015.

41. H. Izadi, A.P. Gerlich. **Distribution and stability of carbon nanotubes during multi-pass friction stir processing of carbon nanotube/aluminum composites**. *Carbon*, Vol.50, no. 12, pp. 4744-4749, 2012.

42. M. Amra, K. Ranjbar, S.A. Hosseini. **Microstructure and wear performance of Al5083/CeO2/SiC mono and hybrid surface composites fabricated by friction stir processing**. *Transactions on Nonferrous Metals Society of China*, Vol. 28, no. 5, pp. 866-878, 2018.

43. G. Huang, W. Hou, Y. Shen. **Evaluation of the microstructure and mechanical properties of WC particle reinforced aluminum matrix composites fabricated by friction stir processing.** *Materials Characterization*, Vol. 138, pp. 26-37, 2018.
44. G. Huang, J. Wu, W. Hou, Y. Shen. **Microstructure, mechanical properties and strengthening mechanism of titanium particle reinforced aluminum matrix composites produced by submerged friction stir processing.** *Material Science and Engineering A*, Vol. 734, pp. 353-363, 2018.
45. A.G. Rao, V.A. Katkar, G. Gunasekaran, V.P. Deshmukh, N. Prabhu, B.P. Kashyap. **Effect of multipass friction stir processing on corrosion resistance of hypereutectic Al-30Si alloy.** *Corrosion Science*, Vol. 83, pp. 198-208, 2014
46. A.K. Srivastava, N.K. Maurya, A.R. Dixit, S.P. Dwivedi, A. Saxena, M. Maurya. **Experimental investigations of A359/Si3N4 surface composite produced by multi-pass friction stir processing.** *Materials Chemistry and Physics*, Vol. 257, ID 123717, 2021.
47. X. Cao, Q. Shi, D. Liu, Z. Feng, Q. Liu, G. Chen. **Fabrication of in situ carbon fiber/aluminum composites via friction stir processing: Evaluation of microstructural, mechanical and tribological behaviors.** *Composites Part B: Engineering*, Vol. 139, pp. 97-105, 2018.
48. V.K.S. Jain, K.U. Yazar, S. Muthukumaran. **Development and characterization of Al5083-CNTs/SiC composites via friction stir processing.** *Journal of Alloys and Compounds*, Vol. 798, pp. 82-92, 2019.
49. N. Nadammal, S.V. Kailas, J. Szpunar, S. Suwas. **Development of microstructure and texture during single and multiple pass friction stir processing of a strain hardenable aluminium alloy.** *Materials Characterization*, Vol. 140, pp. 134-146, 2018.
50. P.M. Sivanesh, P.A. Elaya, S. Arulvel. **Development of multi-pass processed AA6082/SiCp surface composite using friction stir processing and its mechanical and tribology characterization.** *Surface Coatings Technology*, Vol. 394, ID 125900, 2020.
51. M. Nazari, H. Eskandari, F. Khodabakhshi. **Production and characterization of an advanced AA6061-Graphene-TiB2 hybrid surface nanocomposite by multi-pass friction stir processing.** *Surface Coatings Technology*, Vol. 377, ID 124914, 2019.
52. A. Sharma, V.M. Sharma, B. Sahoo, S.K. Pal, J. Paul. **Effect of multiple micro channel reinforcement filling strategy on Al6061-graphene nanocomposite fabricated through friction stir processing.** *Journal of Manufacturing Processes*, Vol. 37, pp. 53-70, 2019.
53. Z. Du, M.J. Tan, J.F. Guo, G. Bi, J. Wei. **Fabrication of a new Al-Al₂O₃-CNTs composite using friction stir processing (FSP).** *Material Science and Engineering A*, Vol. 667, pp. 125-131, 2016.
54. D.R. Ni, J.J. Wang, Z.N. Zhou, Z.Y. Ma. **Fabrication and mechanical properties of bulk NiTip/Al composites prepared by friction stir processing.** *Journal of Alloys and Compounds*, Vol. 586, pp. 368-374, 2014.
55. C.M. Rejil, I. Dinaharan, S.J. Vijay, N. Murugan. **Microstructure and sliding wear behavior of AA6360/(TiC+B4C) hybrid surface composite layer synthesized by friction stir processing on aluminum substrate.** *Material Science and Engineering A*, Vol. 552, pp. 336-344, 2012.
56. J.F. Guo, J. Liu, C.N. Sun, S. Maleksaeedi, G. Bi, M.J. Tan. **Effects of nano-Al₂O₃ particle addition on grain structure evolution and mechanical behaviour of friction-stir-processed Al.** *Material Science and Engineering A*, Vol. 602, pp. 143-149, 2014.
57. A. Sharma, H. Fujii, J. Paul. **Influence of reinforcement incorporation approach on mechanical and tribological properties of AA6061- CNT nanocomposite fabricated via FSP.** *Journal of Manufacturing Processes*, Vol. 59, pp. 604-620, 2020.
58. N. Netto, L. Zhao, J. Soete, G. Pyka, A. Simar. **Manufacturing high strength aluminum matrix composites by friction stir processing: An innovative approach.** *Journal of Materials Processing Technology*, Vol. 283, ID 116722, 2020.
59. H.G. Rana, V.J. Badheka, A. Kumar. **Fabrication of Al7075 / B4C Surface Composite by Novel Friction Stir Processing (FSP) and Investigation on Wear Properties.** *Procedia Technology*, Vol. 23, pp. 519-528, 2016.
60. F. García-Vázquez, B. Vargas-Arista, R. Muñiz R, J.C. Ortiz, H.H. García, J. Acevedo. **The Role of Friction Stir Processing (FSP) Parameters on TiC Reinforced Surface Al7075-T651 Aluminum Alloy.** *Soldagem & Inspecao*, Vol 21, no. 4, 508-516, 2016.
61. R. Ande, P. Gulati, K.D. Shukla, H. Dhingra. **Microstructural and Wear Characteristics of Friction Stir Processed Al-7075/SiC Reinforced Aluminium Composite.** *Materials Today: Proceedings*, Vol. 18, pp. 4092-4101, 2019.
62. Z.Y. Liu, B.L. Xiao, W.G. Wang, Z.Y. Ma. **Analysis of carbon nanotube shortening and composite strengthening in carbon nanotube/aluminum composites fabricated by multi-pass friction stir processing.** *Carbon*, Vol. 69, pp. 264-274, 2014.
63. Z.W. Zhang, Z.Y. Liu, B.L. Xiao, D.R. Ni, Z.Y. Ma. **High efficiency dispersal and strengthening of graphene reinforced aluminum alloy composites fabricated by powder metallurgy combined with friction stir processing.** *Carbon*, Vol. 135, pp. 215-223, 2018.
64. S.M. Khorrami, M. Kazeminezhad, A.H. Kokabi. **The effect of SiC nanoparticles on the friction stir processing of severely deformed aluminum.** *Material Science and Engineering A*, Vol. 602, pp. 110-118, 2014.
65. S.M. Khorrami, S. Samadi, Z. Janghorban, M. Movahedi. **In-situ aluminum matrix composite produced by friction stir processing using FE particles.** *Material Science and Engineering A*, Vol. 641, pp. 380-390, 2015.
66. J. Wang, X. Lu, C. Cheng, B. Li, Z.Y. Ma. **Improve the quality of 1060Al/Q235 explosive composite plate by friction stir processing.** *Journal of Materials Research and Technology*, Vol. 9, no. 1, pp. 42-51, 2020.

67. Q. Liu, L. Ke, F. Liu, C. Huang, L. Xing. **Microstructure and mechanical property of multi-walled carbon nanotubes reinforced aluminum matrix composites fabricated by friction stir processing.** *Materials and Design*, Vol. 45, pp. 343-348, 2013.
68. Y. Zhao, Z. Ding, Y. Chen. **Crystallographic orientations of intermetallic compounds of a multi-pass friction stir processed Al/Mg composite materials.** *Materials Characterization*, Vol. 128, pp. 156-164, 2017.
69. M.Z.M. Kotiyani, K. Ranjbar, R. Dehmolaei. **In-situ fabrication of Al₃Zr aluminide reinforced AA3003 alloy composite by friction stir processing.** *Materials Characterization*, Vol. 131, pp. 78-90, 2017.
70. M. Golmohammadi, M. Atapour, A. Ashrafi. **Fabrication and wear characterization of an A413/Ni surface metal matrix composite fabricated via friction stir processing.** *Materials and Design*, Vol. 85, pp. 471-482, 2015.
71. H. Eskandari, R. Taheri, F. Khodabakhshi. **Friction-stir processing of an AA8026-TiB₂-Al₂O₃ hybrid nanocomposite: Microstructural developments and mechanical properties.** *Material Science and Engineering A*, Vol. 660, pp. 84-96, 2016.
72. M.M. El-Rayes, E.A. El-Danaf. **The influence of multi-pass friction stir processing on the microstructural and mechanical properties of Aluminum Alloy 6082.** *Journal of Materials Processing Technology*, Vol. 212, no. 5, pp. 1157-1168, 2012.
73. K. Nakata, Y.G. Kim, H. Fujii, T. Tsumura, T. Komazaki. **Improvement of mechanical properties of aluminum die casting alloy by multi-pass friction stir processing.** *Material Science and Engineering A*, Vol. 437, no. 2, pp. 274-280, 2006.
74. K.J. Al-Fadhlah, A.I. Almazrouee, A.S. Aloraier. **Microstructure and mechanical properties of multi-pass friction stir processed aluminum alloy 6063.** *Materials and Design*, Vol. 53, pp. 550-560, 2014.
75. Y. Chen, H. Ding, S. Malopheyev, R. Kaibyshev, Z. Cai, W. Yand. **Influence of multi-pass friction stir processing on microstructure and mechanical properties of 7B04-O Al alloy.** *Transactions of Nonferrous Metals Society of China*, Vol. 27, no. 4, pp. 789-796, 2017.
76. S. Meenia, F.K. MD, S. Babu, R.J. Immanuel, S.K. Panigrahi, G.D.J. Ram. **Particle refinement and fine-grain formation leading to enhanced mechanical behaviour in a hypo-eutectic Al-Si alloy subjected to multi-pass friction stir processing.** *Materials Characterization*, Vol. 113, pp. 134-143, 2016.
77. Y. Chen, H. Ding, J. Li, Z. Cai, J. Zhao, W. Yang. **Influence of multi-pass friction stir processing on the microstructure and mechanical properties of Al-5083 alloy.** *Material Science and Engineering A*, Vol. 650, pp. 281-289, 2016.
78. S. Jana, R.S. Mishra, J.A. Baumann, G. Grant. **Effect of process parameters on abnormal grain growth during friction stir processing of a cast Al alloy.** *Material Science and Engineering A*, Vol. 528, pp. 189-199, 2010.
79. S.K. Singh, R.J. Immanuel, S. Babu, S.K. Panigrahi, J.G.D. Ram. **Influence of multi-pass friction stir processing on wear behaviour and machinability of an Al-Si hypoeutectic A356 alloy.** *Journal of Materials Processing Technology*, Vol. 236, pp. 252-262, 2016.
80. A.G. Rao, V.A. Katkar, G. Gunasekaran, V.P. Deshmukh, N. Prabhu, B.P. Kashyap. **Effect of multipass friction stir processing on corrosion resistance of hypereutectic Al-30Si alloy.** *Corrosion Science*, Vol. 83, pp. 198-208, 2014.
81. K.N. Ramesh, S. Pradeep, V. Pancholi. **Multipass Friction-Stir Processing and its Effect on Mechanical Properties of Aluminum Alloy 5086.** *Metallurgical and Materials Transactions A*, Vol. 43, no. 11, pp. 4311-4319, 2012.
82. H. Vyas, K.P. Mehta. **Effect of Multi Pass Friction Stir Processing on Surface Modification and Properties of Aluminum Alloy 6061.** *Key Engineering Materials*, Vol. 813, pp. 404-410, 2019.
83. N. Saini, C. Pandey, D.K. Dwivedi. **Ductilizing of cast hypereutectic Al-17%Si alloy by friction stir processing.** *Proceedings of the Institution of Mechanical Engineers, Part E: Journal of Process Mechanical Engineering*, Vol.232, no. 6, pp. 696-701, 2018.
84. J.L. Baruch, R. Raju, V. Balasubramanian, A.G. Rao, I. Dinaharan. **Influence of multi-pass friction stir processing on microstructure and mechanical properties of die cast Al-7Si-3Cu aluminum alloy.** *Acta Metallurgica Sinica (English Lett.)*, Vol. 29, no. 5, pp. 431-440, 2016.
85. N. Saini, D.K. Dwivedi, P.K. Jain, H. Singh. **Surface Modification of Cast Al-17%Si Alloys Using Friction Stir Processing.** *Procedia Engineering*, Vol. 100, pp.1522-1531, 2015
86. R. Prasad, S.P. Tewari, J.K. Singh. **Effect of multi-pass friction stir processing on microstructural, mechanical and tribological behaviour of as-cast Al-Zn-Mg-Cu alloy.** *Material Research Express*, Vol. 6, no. 9, ID 96579, 2019.
87. S. Mabuwa, V. Msomi. **Fatigue behaviour of the multi-pass friction stir processed AA8011-H14 and AA6082-T651 dissimilar joints.** *Engineering Failure Analysis*, Vol. 118, ID 104876, 2020.
88. S. Mabuwa, V. Msomi. **The Influence of Multiple Pass Submerged Friction Stir Processing on the Microstructure and Mechanical Properties of the FSWed AA6082-AA8011 Joints.** *Metals*, Vol. 10, ID 1429, 2020.